Assessing Urban Methane Emissions with Satellite-Derived Enhancement Ratios

Jon-Paul Mastrogiacomo[1], Cameron G. MacDonald[2], Coleen M. Roehl[3], Paul O. Wennberg[3], Debra Wunch[1]

1 University of Toronto, Toronto, Ontario 2 Princeton University, Princeton, New Jersey, 3 California Institute of Technology, Pasadena, California

Contact: jp.mastrogiacomo@mail.utoronto.ca

Introduction

Methane emission mitigation has been at the forefront of policy discussion in recent years due to its short atmospheric lifetime and large global warming potential. COP26 saw the launch of the Global Methane Pledge in which more than 155 countries responsible for over 50% of total anthropogenic methane emissions pledge to reduce emissions by 30% below 2020 levels by 2030. Urban areas are a particular focus of mitigation policy as emissions are often from point sources (e.g., landfills, wastewater treatment plants) and can be addressed by local governments or made to be profitable (e.g., natural gas fugitive emissions).

But emissions from urban sources are difficult to characterize by bottom-up methods as they are often intermittent and vary significantly site-to-site. Aircraft and ground-based measurement campaigns in several US cities have found notable underestimates of methane emissions. Satellite measurements offer a means to evaluate emissions from global cities with a consistent methodology over the span of many years.

Objectives and Materials

We calculate methane enhancement ratios from satellite measurements for cities across the world, building on the methodology of MacDonald et al. (2023). We compare them to emissions ratios calculated from a variety of globally-gridded inventories. We also combine our satellite enhancement ratios with inventory emissions to estimate annual urban CH_4 emissions.

Methane (CH_4), carbon monoxide (CO), and nitrogen dioxide (NO_2) measurements are provided by the TROPOspheric Monitoring Instrument (TROPOMI; Veefkind et al., 2012). We use the operational TROPOMI products, plus an additional CH_4 product based on the Weighting Function Modified Differential Optical Absorption Spectroscopy (WFMD) retrieval algorithm (Schneising et al., 2023).

Carbon dioxide (CO_2) measurements are provided by NASA's Orbiting Carbon Observatory 2 (OCO-2; Crisp et al., 2004) and Orbiting Carbon Observatory 3 (OCO-3; Eldering et al., 2019). We use the OCO-3 SAM and OCO-2/3 Nadir modes but exclude Target and Glint modes.

Emissions of CH_4, CO, and CO_2 are taken from the Emissions Database for Global Atmospheric Research v8 (EDGAR; Crippa et al., 2023) and from the Global Anthropogenic Emissions for the Copernicus Atmosphere Monitoring Service v6.2 (CAMS_GLOB_ANT; Soulie et al., 2024). We also use CO emissions from of the Task Force on Hemispheric Transport of Air Pollution (HTAP) inventory v3 (Crippa et al., 2023), and national CH_4 emissions inventories for the USA (Maasakkers et al., 2023) and Mexico (Scarpelli et al., 2020).

City polygons, areas, and populations taken from the European Commission Joint Research Centre's Global Human Settlement Urban Centre Database version R2019A (Florczyk et al. 2019).

References

Crippa, M., et al. (2023). Insights on the Spatial Distribution of Global, National and Sub-National GHG Emissions in EDGARv8.0. *Earth System Science Data Discussions* 1–28. doi: 10.5194/essd-2023-514.
Crippa, M., et al. (2023). The HTAP_v3 Emission Mosaic: Merging Regional and Global Monthly Emissions (2000–2018) to Support Air Quality Modelling and Policies. *Earth System Science Data* 15(6):2667–94. doi: 10.5194/essd-15-2667-2023.
Eldering, A., et al. (2019). The OCO-3 Mission: Measurement Objectives and Expected Performance Based on 1 Year of Simulated Data. *Atmospheric Measurement Techniques* 12(4):2341–70. doi: 10.5194/amt-12-2341-2019.
Crisp, D., et al. (2004). The Orbiting Carbon Observatory (OCO) Mission. *Advances in Space Research* 34(4):700–709. doi: 10.1016/j.asr.2003.08.062.
Florczyk A., et al. (2019) GHS Urban Centre Database 2015, multitemporal and multidimensional attributes, R2019A. *European Commission, Joint Research Centre (JRC)*.
Laughner, J. L., et al. (2024). Report: TCCON GGG2020 switch to GEOS IT met products. CaltechDATA. https://doi.org/10.14291/tccon.ggg2020.report.geosit-change.
Maasakkers, J. D., et al. (2023). A Gridded Inventory of Annual 2012–2018 U.S. Anthropogenic Methane Emissions. *Environmental Science & Technology* 57(43):16276–88. doi: 10.1021/acs.est.3c05138.
MacDonald, C. G., (2023). Estimating Enhancement Ratios of Nitrogen Dioxide, Carbon Monoxide and Carbon Dioxide Using Satellite Observations. *Atmospheric Chemistry and Physics* 23(6):3493–3516. doi: 10.5194/acp-23-3493-2023.
Plant, G, et al., (2022). Evaluating Urban Methane Emissions from Space Using TROPOMI Methane and Carbon Monoxide Observations. *Remote Sensing of Environment* 268:112756. doi: 10.1016/j.rse.2021.112756.
Scarpelli, T. R., (2020). A Gridded Inventory of Anthropogenic Methane Emissions from Mexico Based on Mexico's National Inventory of Greenhouse Gases and Compounds. *Environmental Research Letters* 15(10):105015. doi: 10.1088/1748-9326/abb42b.
Schneising, O., (2023). Advances in Retrieving XCH4 and XCO from Sentinel-5 Precursor: Improvements in the Scientific TROPOMI/WFMD Algorithm. *Atmospheric Measurement Techniques* 16(3):669–94. doi: 10.5194/amt-16-669-2023.
Soulie, A., et al. (2024). Global Anthropogenic Emissions (CAMS-GLOB-ANT) for the Copernicus Atmosphere Monitoring Service Simulations of Air Quality Forecasts and Reanalyses. Earth System Science Data 16(5):2261–79. doi: 10.5194/essd-16-2261-2024.
Veefkind, J. P., et al. (2012). TROPOMI on the ESA Sentinel-5 Precursor: A GMES Mission for Global Observations of the Atmospheric Composition for Climate, Air Quality and Ozone Layer Applications. *Remote Sensing of Environment* 120:70–83. doi: 10.1016/j.rse.2011.09.027.
Wennberg, P. O., et al. (2022). TCCON data from Caltech (US), Release GGG2020.R0 (Version R0) [Data set]. CaltechDATA. https://doi.org/10.14291/tccon.ggg2020.pasadena01.R0.
Wunch, D., et al. (2009). Emissions of Greenhouse Gases from a North American Megacity. *Geophysical Research Letters* 36(15). doi: 10.1029/2009GL039825.

Methodology

1. Identify TROPOMI CH_4 overpasses over a given city coincident with those of other species. We consider OCO-2/3 nadir tracks within 75km. We consider OCO-3 SAMs and nadir tracks within 3 hours. We consider every pair of TROPOMI CH_4 and CO overpasses.
2. Identify enhancement pixels
   - For OCO-2/3 nadir overpasses downwind of the city, use intersection of modelled Gaussian plume and ground track.
   - For all other cases, use TROPOMI NO_2 plume. Calculate XNO_2 anomalies and select pixels above 95th percentile. Find intersection between these pixels and other two species (Figure 1, bottom-right).

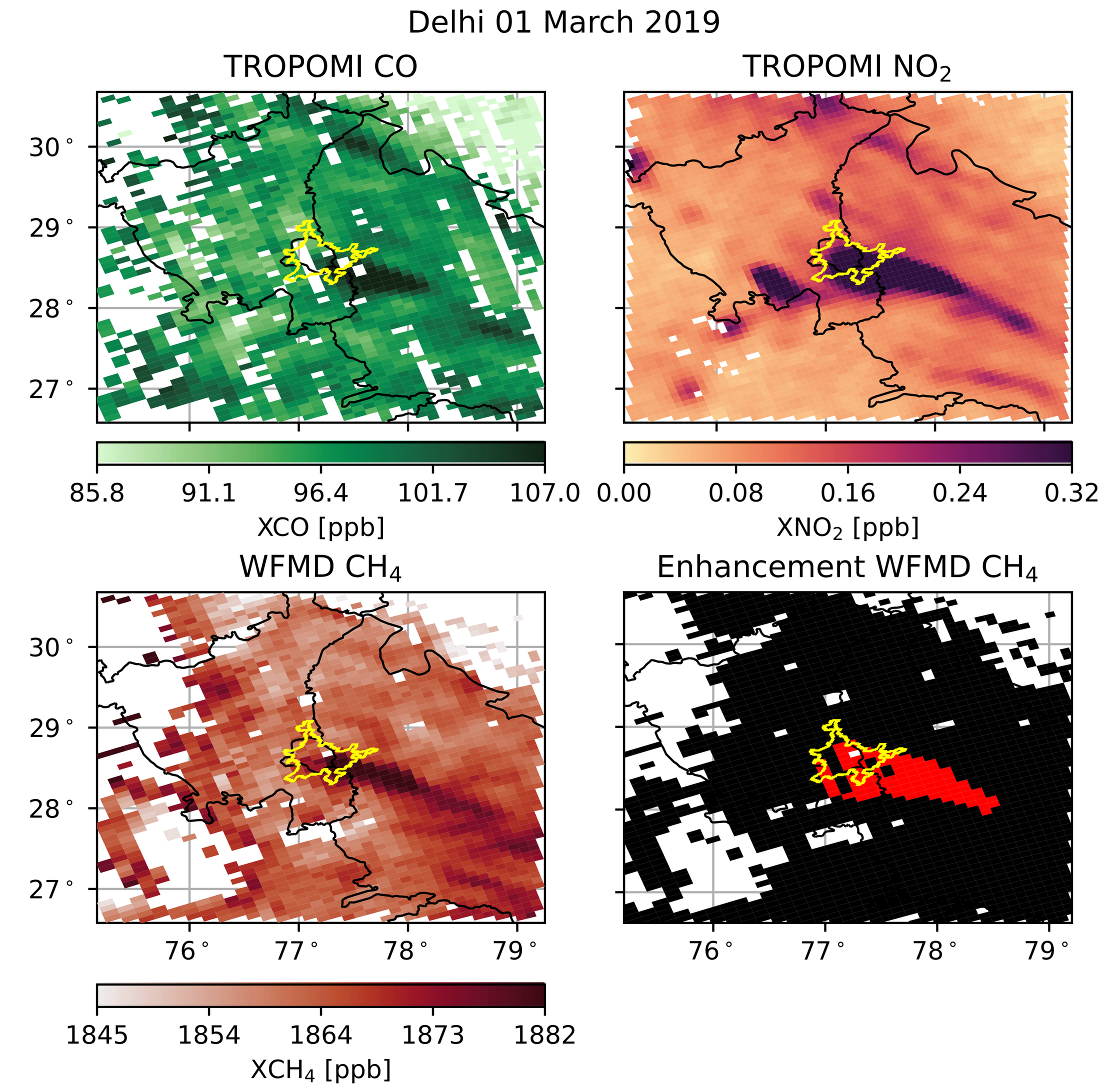

Figure 1: TROPOMI XCO (top-left), XNO_2 (top-right), and XCH_4 (bottom-left) measurements take over Delhi India on 2019-03-01. Red XCH_4 pixels identified as enhancement pixels (bottom-right).

3. Smooth overpasses with a nearest-neighbour fit of radius 2 seconds (OCO-2/3 nadir), 5 km (OCO-3 SAMs), or 12 km (TROPOMI).
4. Calculate background surfaces with a nearest-neighbour fit of radius 20 seconds (OCO-2/3 nadir), 100 km (OCO-3 SAMs), or 150 km (TROPOMI). Subtract background from smoothed overpasses to derive anomalies.
5. From anomalies, subtract contribution due to urban-rural gradient in TROPOMI priors and divide by surface averaging kernel:
$$\Delta c^t = \frac{\Delta \hat{c}}{a^0} - \frac{(1-a^0)(c_u^a - c_b^a)}{a^0}$$
where Δc^t is the true enhancement, $\Delta \hat{c}$ is the retrieved enhancement, a^0 is the surface layer of the column averaging kernel, and c_u^a / c_u^b are the a priori urban and background columns.
6. Calculate enhancement ratio for all overpasses simultaneously with a reduced major axis regression (Figure 2).

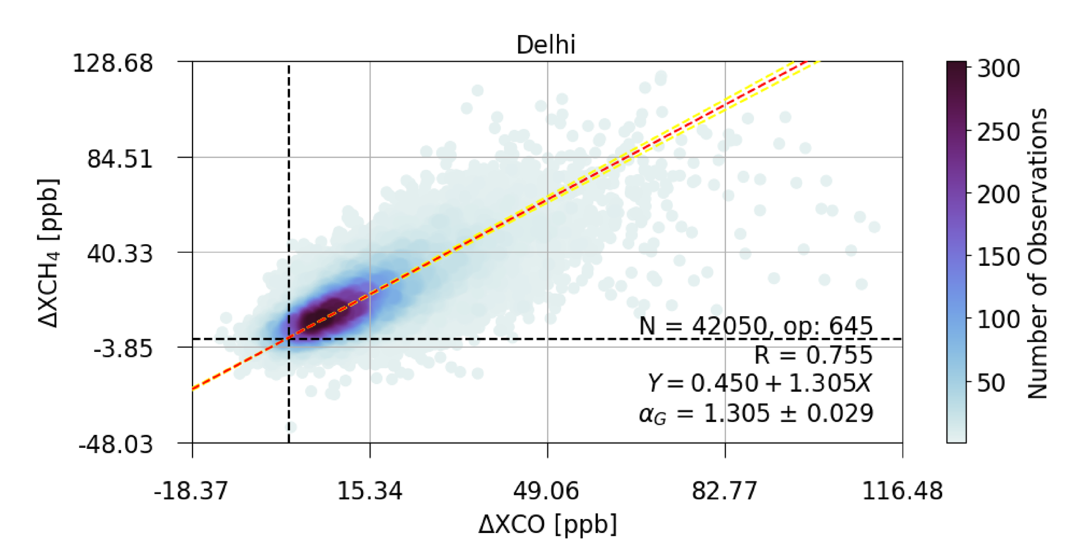

Figure 2: Reduced major axis regression of all XCH_4 and XCO anomalies over Delhi, India.

Results

We calculate CH_4 : CO enhancement ratios for a select 10 cities using both the TROPOMI and WFMD CH_4 products (Figure 3). We also calculate emissions ratios from 3 CH_4 and 3 CO globally-gridded inventories. We see reasonable agreement with a subset of inventories in most cities. However, there are significant discrepancies between inventories.

In some cities (Ahmadabad, Delhi, Dhaka, Karachi) we see better overall agreement with EDGAR CH_4 emissions than with CAMS_GLOB_ANT CH_4 emissions. However, the opposite is true in Al Ain. CO emissions in HTAP are always similar to those in CAMS_GLOB_ANT, while EDGAR CO can deviate significantly (Al Ain, Buenos Aires, Dhaka).

The U.S. National CH_4 inventory agrees better with measurements than EDGAR or CAMS_GLOB_ANT in Washington D.C. and Los Angeles. But the Mexico National CH_4 inventory seems to perform worse in Mexico City and Monterrey, possibly because emissions are based on 2015 values.

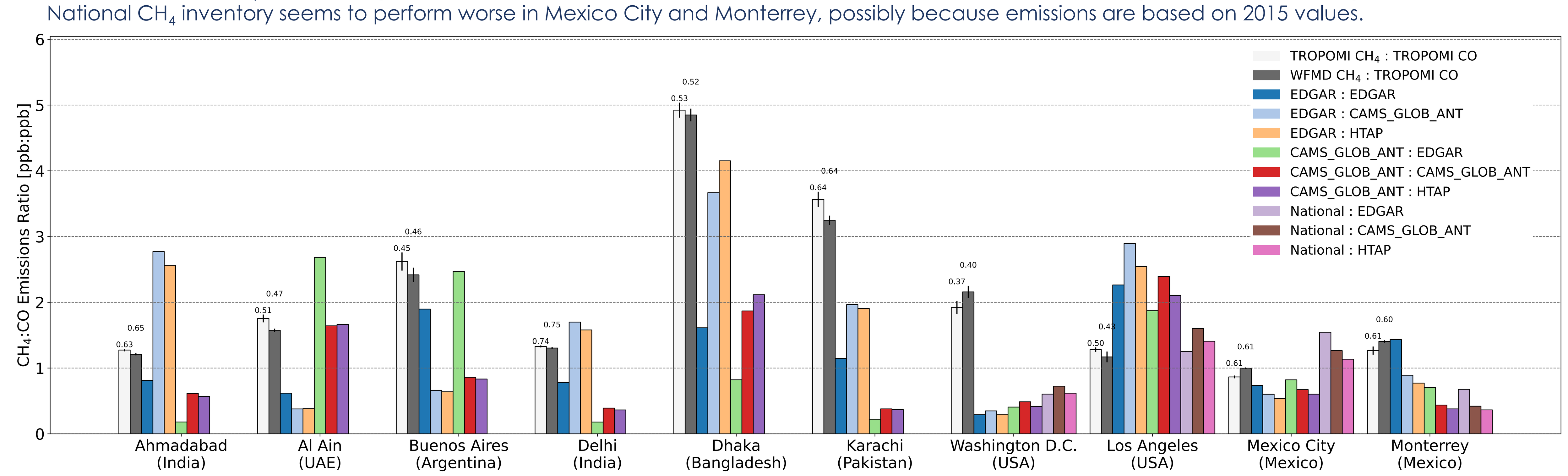

Figure 3: CH_4 : CO enhancement and emissions ratios derived from satellite and inventories. Values above the bars are Pearson correlation coefficients.

Given our satellite-derived CH_4 : CO_2 ratio ($\alpha^{Sat}_{CH4:CO2}$), we calculate CH_4 emissions as

$$E^{Sat}_{CH4} = \alpha^{Sat}_{CH4:CO2} \cdot E^{Inv}_{CO2} \cdot \frac{M_{CH4}}{M_{CO2}}$$

where E^{Inv}_{CO2} is given by a CO_2 emission inventory and M_{CH4} and M_{CO2} are the molar masses of CH_4 and CO_2.

Emissions estimates can be used to compare. We see an inverse relationship between Emissions per capita and Population density (Figure 4). However, there are notable outliers with both high per capita emissions and high population densities. North American cities consistently have the highest per capita methane emissions.

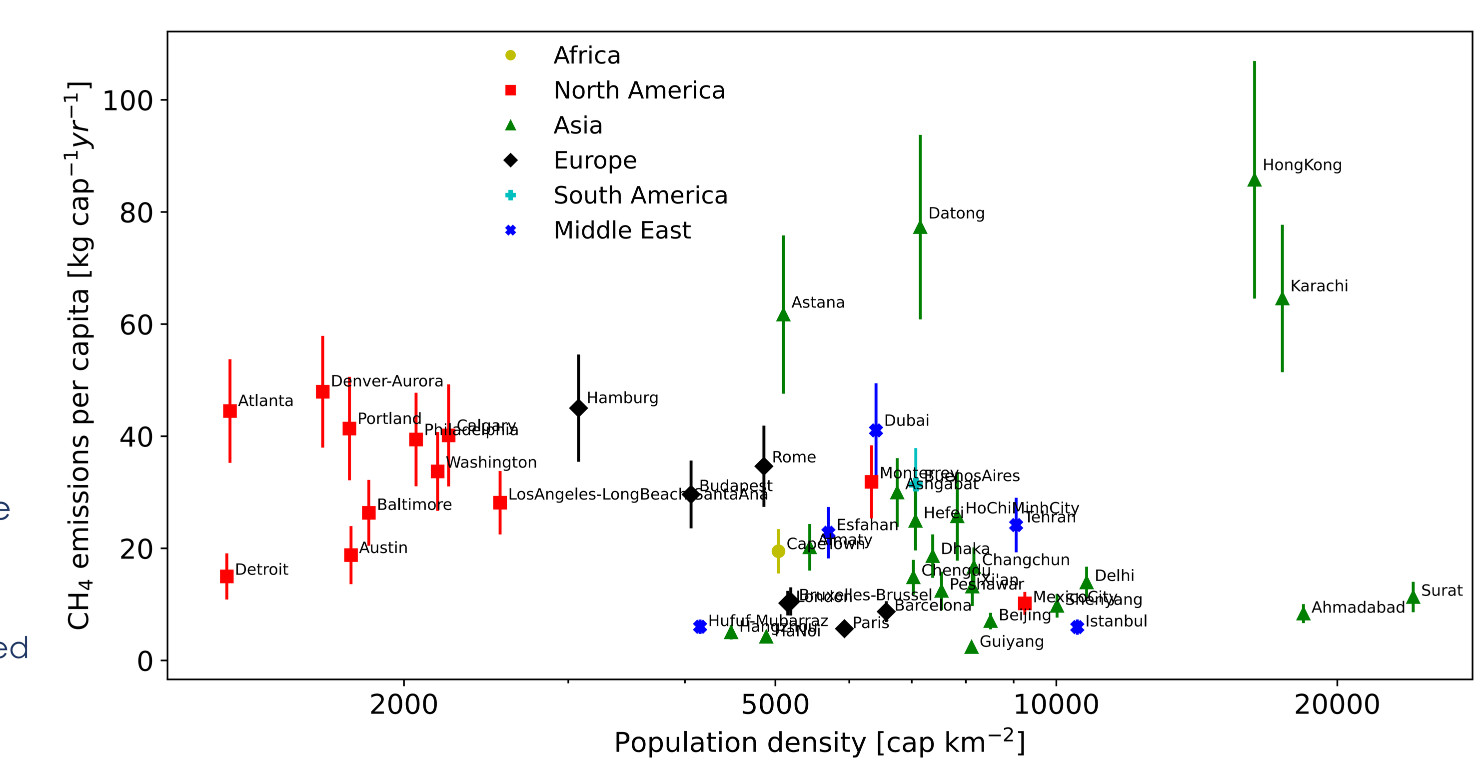

Figure 4: CH_4 emissions per capita calculated with satellite-derived TROPOMI CH_4 : CO_2 ratio and EDGAR CO_2 emissions. Population density calculated as built-up area divided by total population (plotted on logarithmic scale).

Comparisons

We compare our CH_4 : CO enhancement ratios to those derived in Plant et al. (2022) using a different methodology (Figure 5). The ratios agree within uncertainty in 5/11 cities, although the uncertainty on our enhancement ratios is underestimated. Values for some cities have low correlation coefficients due to poor TROPOMI CH_4 coverage.

We also calculate a CH_4 : CO enhancement ratio using measurements from the ground-based Caltech TCCON station (Wennberg et al., 2022). We use the GGG2014 product due to a known issue with the GGG2020 CO priors in Los Angeles (Laughner et al., 2024). We follow the methodology of Wunch et al. (2009) and see good agreement with our satellite-derived ratio.

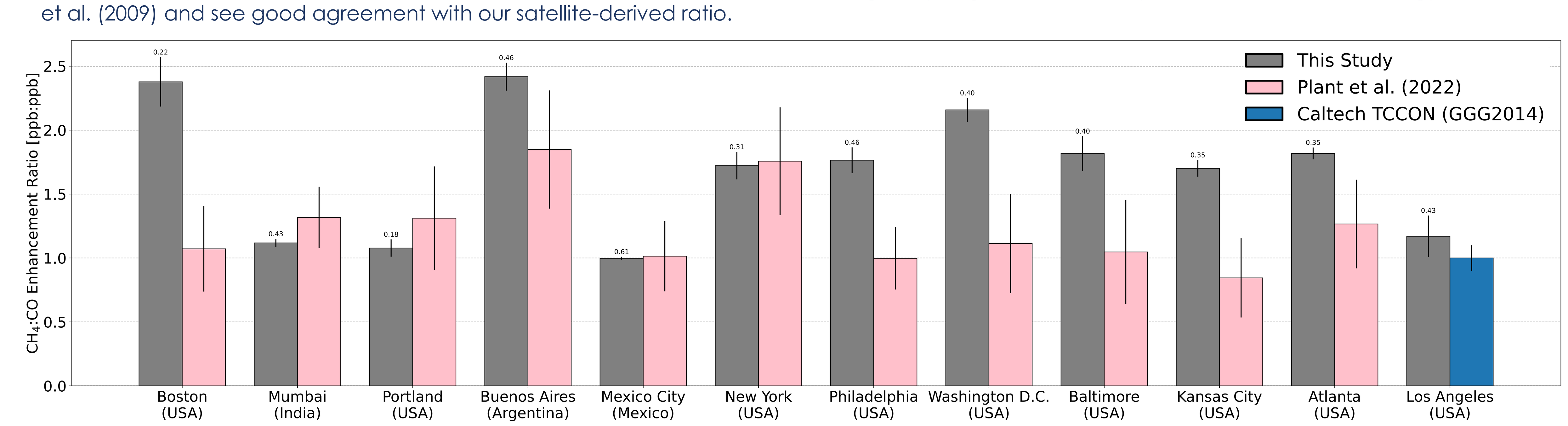

Figure 5: WFMD CH_4 : CO enhancement ratios in our study compared to those in Plant et al. (2022) and to the Caltech TCCON station. Values above the bars are Pearson correlation coefficients.